Green synthesis, optical properties and catalytic activity of silver nanoparticles in the synthesis of *N*-monosubstituted ureas in water

Mahmoud Nasrollahzadeh[a,*], Ferydon Babaei[b], S. Mohammad Sajadi[c] and Ali Ehsani[a]

[a] *Department of Chemistry, Faculty of science, University of Qom, P. O. Box 37185-359, Qom, Iran.*
[b] *Department of Physics, Faculty of Science, University of Qom, Qom, Iran.*
[c] *Department of Petroleum Geoscience, Faculty of Science, Soran University, PO Box 624, Soran, Kurdistan Regional Government, Iraq*
*Corresponding author. Tel: +98 253 32850953; Fax: +98 253 32103595.
E-mail address: mahmoudnasr81@gmail.com

ABSTRACT

We report the green synthesis of silver nanoparticles by using *Euphorbia condylocarpa M. bieb* root extract for the synthesis of *N*-monosubstituted ureas in water. UV-Visible studies show the absorption band at 420 nm due to surface plasmon resonance (SPR) of the silver nanoparticles. This reveals the reduction of silver ions (Ag^{+}) to silver (Ag^{o}) which indicates the formation of silver nanoparticles (Ag NPs). This method has the advantages of high yields, simple methodology and easy work up.

Keywords: UV-Visible, *N*-Monosubstituted urea, Surface plasmon resonance, Ag nanoparticles, Euphorbia condylocarpa M. bieb

1. Introduction

N-Monosubstituted ureas have potential medical and agricultural applications [1,2]. Several methods for their preparation have been reported, but synthetic approaches for these compounds are needed. Classical methods for the synthesis of *N*-monosubstituted ureas have involved reaction of primary or secondary amines with isocyanates [3,4], toxic phosgene or its derivatives [5,6], insertion of CO or CO_2 into amino compounds in the presence of different catalysts in organic solvents at high temperature and pressure [7-10], reaction of amines with sodium or potassium cyanate in aqueous solution in the presence of one equivalent of HCl [11], acid or base-catalyzed hydration of cyanamides [12-15], and reaction of *S*,*S*-dimethyl dithiocarbonate with ammonia in water-dioxane [16].

Earlier reported methods for the preparation of *N*-monosubstituted ureas suffer from drawbacks such as the use of expensive and toxic reagents and catalysts, the environmental pollution caused by utilization of organic solvents and use of corrosive base or acids such as HF-pyridine complex, H_2SO_4, H_2O_2/NaOH and HCl, low yields, high temperatures, long reaction times, harsh reaction conditions, difficulty in availability or preparing the starting materials or catalysts, tedious work-up, waste control and

formation of side products. Therefore, the need for ógreenerô methods or chemical products that reduce or eliminate the use and generation of hazardous compounds is essential.

Among currently available synthetic routes to *N*-monosubstituted ureas, the most widely used one is based upon hydration of cyanamides [12-15], which involves the treatment of cyanamides with corrosive acids or bases. To resolve this problem, recently Kim et al. described the hydration of cyanamides into ureas using $InCl_3$ and acetaldoxime as a water surrogate in toluene as the toxic organic solvent [17]. However, the development of an efficient and versatile method for the hydration of cyanamides is an active ongoing research area, and there is a potential for further improvement toward green chemistry.

From the standpoint of ógreen chemistryô and for reasons of economy and pollution, organic reactions in water are of great interest to make the classical procedures more clean, safe and easy to perform [18,19]. Water is cheap, non-toxic, non-combustible, non-explosive, and environmentally acceptable [18,19].

Nanotechnology is emerging as a cutting edge technology interdisciplinary with biology, chemistry and material science. In recent years, noble metal nanoparticles have been the subjects of focused researches due to their unique electronic, optical, mechanical, magnetic and chemical properties that are significantly different from those of bulk materials [20]. For these reasons, metallic nanoparticles have found uses in many applications in different fields, such as catalysis, photonics, and electronics.

In nanotechnology, silver nanoparticles are the most promising one. Silver nanoparticles (Ag NPs) have been widely used during the past few years in various applications, such as biomedicine, biosensors, catalysis, pharmaceuticals, electrical conductivity, photonics and as the substrates for surface-enhanced Raman spectroscopy (SERS) due to the existence of surface plasmons [21-26]. The silver nanoparticles provide high surface energy, which promotes surface reactivity (e.g., adsorption, catalysis). One unique property of silver nanoparticles includes their utilization in fluorescence and surface plasmon resonance (SPR) [23,24,27]. The frequency and intensity of plasmon resonance are dependent on the distribution of charge across the nanostructure, which in turn is determined by the shape [28].

Hence in recent years the green synthesis approach has emerged as one of the active areas of research. The green synthesis techniques are generally synthetic routes that utilize relatively nontoxic solvents such as water, biological extracts, biological systems and microwave assisted synthesis [29-35]. Green synthesis of NPs has several advantages over chemical synthesis, such as simplicity, cost effectiveness as well as compatibility for biomedical and pharmaceutical applications.

The plants of the *Euphorbiaceae* contain acrid, milky, or colorless juice. Chemical data are available for several genera, especially Eubhorbia, where more than 120 species have been investigated. The family *Euphorbiaceae* is rich in flavonoids, particularly

flavones and flavonols, which have been identified from several genera. Furthermore, the previouse studies in 1970 on *Euphorbia condylocarpa* demonstrated the presence of phytochemicals such as flavonoids, tetracyclic triterpenoids, and trifolin in different parts of the plant [33-36].

In continuation of our recent works on the green chemistry [36-40], we wish to report a new and rapid protocol for the preparation of silver nanoparticles by using *Euphorbia condylocarpa M. bieb* root extract (Figure 1) as a reducing and stabilizing agent. Also, the optical absorption properties was measured by UV-Visible spectrophotometer and observed the absorption peak in 440 nm region due to surface plasmon resonance (SPR) of the silver nanoparticles.

Figure 1. Image of *Euphorbia condylocarpa M. bieb***.**

In addition, we hereby report a new protocol for the hydration of cyanamides in water using silver nanoparticles as a stable heterogeneous catalyst (Scheme 1).

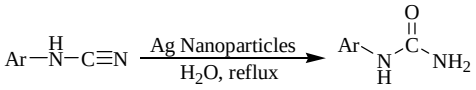

Scheme 1

2. Experimental and modeling

All reagents were purchased from the Merck and Aldrich chemical companies and used without further purification. Products were characterized by different spectroscopic methods (FT-IR and NMR spectra), elemental analysis (CHN) and melting points. The NMR spectra were recorded in acetone and DMSO. ^{1}H NMR spectra were recorded on a Bruker Avance DRX 250, 300 and 400 MHz instrument. The chemical shifts (δ) are reported in ppm relative to the TMS as internal standard. *J* values are given in Hz. IR (KBr) spectra were recorded on a Perkin-Elmer 781 spectrophotometer. Melting points were taken in open capillary tubes with a BUCHI 510 melting point apparatus and were

uncorrected. The elemental analysis was performed using Heraeus CHN-O-Rapid analyzer. TLC was performed on silica gel polygram SIL G/UV 254 plates. UV-Visible spectral analysis was recorded on a double-beam spectrophotometer (Hitachi, U-2900) to ensure the formation of nanoparticles.

2.1. General procedure for the synthesis of cyanamides

Cyanamides were prepared according to the literature [41].

2.2. Preparation of Euphorbia condylocarpa M. bieb root extract

10 G of dried plant powder was extracted using boiling in 100 mL double distillated water for 10 min and aqueous extract was filtered.

2.3. Green synthesis of silver nanoparticles using Euphorbia condylocarpa M. bieb root extract

In a typical synthesis of Ag NPs, 5 mL of aqueous extract was added dropwise to 50 mL of 0.003 M aqueous solution of $AgNO_3$ (0.003 M) with constant stirring at 50 °C. After 30 min the color of the solution changed from yellow to reddish brown during the heating process due to excitation of surface plasmon resonance which indicates the formation of Ag nanoparticles. Reduction of silver ions (Ag^+) to silver (Ag^o) was completed around 1 hour (as monitored by UV-Vis and FT-IR spectra of the solution). Then the colored solution of silver nanoparticles was centrifuged at 6000 rpm for 30 min to completely dispersing. The nanoparticles solution was diluted 10 times with distilled water to avoid the errors due to high optical density of the solution.

2.4. General procedure for the hydration of cyanamides to N-monosubstituted ureas using silver nanoparticles

A mixture of the appropriate cyanamide (1.0 mmol), water (10 mL) and Ag NPs (5.0 mg) was stirred under reflux conditions for 1 h. After completion of reaction (as monitored by TLC), Ag NPs were separated from the reaction mixture by centrifugation. The desired pure products were characterized by ^{1}H NMR, ^{13}C NMR, FT-IR, elemental analysis (CHN), and melting points.

2.5. Spectra Data

***N*-Phenylurea** (Table 2, entry 1): M.p. 143-145 °C; FT-IR (KBr, cm^{-1}) 3346, 3268, 3243, 3193, 3057, 1740, 1656, 1597, 1561, 1493, 1447, 1369, 1319, 1238, 1068, 737, 691, 605, 491; ^{1}H NMR (300 MHz, DMSO-d_6) δ_H = 8.55 (s, 1H), 7.38 (d, J = 7.8 Hz, 2H), 7.20 (t, J = 7.6 Hz, 2H), 6.87 (t, J = 7.2 Hz, 1H), 5.84 (s, 2H); ^{13}C NMR (75 MHz, DMSO-d_6) δ_C = 156.5, 141.0, 129.0, 121.5, 118.2; Anal. Calcd for $C_7H_8N_2O$: C, 61.75; H, 5.92; N, 20.58. Found: C, 61.65; H, 5.82; N, 20.49.

***N*-(4-Methoxyphenyl)urea** (Table 2, entry 2): M.p. 167-169 °C; FT-IR (KBr, cm^{-1}) 3471, 3337, 3195, 2955, 2837, 1645, 1616, 1592, 1547, 1512, 1417, 1347, 1302, 1247, 1137, 1108, 1038, 823, 785, 675, 563, 519; ^{1}H NMR (300 MHz, DMSO-*d*$_6$) δ_H = 8.27 (s, 1H), 7.26 (d, *J* = 7.2 Hz, 2H), 6.78 (d, *J* = 7.2 Hz, 2H), 5.68(s, 2H), 3.67 (s, 3H); ^{13}C NMR (75 MHz, DMSO-*d*$_6$) δ_C = 156.6, 154.3, 134.1, 119.9, 114.3, 55.6; Anal. Calcd for $C_8H_{10}N_2O_2$: C, 57.82; H, 6.07; N, 16.86. Found: C, 57.71; H, 5.94; N, 16.78.

***N*-(4-Methylphenyl)urea** (Table 2, entry 3): M.p. 182-184 °C; FT-IR (KBr, cm^{-1}) 3431, 3311, 3041, 2920, 1655, 1620, 1591, 1551, 1514, 1408, 1357, 1256, 1109, 1024, 824, 811, 708, 638, 551, 501; ^{1}H NMR (300 MHz, DMSO-*d*$_6$) δ_H = 8.35 (s, 1H), 7.24 (d, *J* = 7.8Hz, 2H), 7.00 (d, *J* = 7.8Hz, 2H), 5.73 (s, 2H), 2.20 (s, 3H); ^{13}C NMR (75 MHz, DMSO-*d*$_6$) δ_C = 156.5, 138.4, 130.1, 129.4, 118.2, 20.7; Anal. Calcd for $C_8H_{10}N_2O$: C, 63.98; H, 6.71; N, 18.65. Found: C, 63.35; H, 6.65; N, 18.51.

***N*-(2-Methylphenyl)urea** (Table 2, entry 4): M.p. 198-200 °C; FT-IR (KBr, cm^{-1}) 3438, 3315, 3218, 1650, 1613, 1582, 1547, 1459, 1354, 1289, 1258, 1117, 1041, 844, 747, 596, 480; ^{1}H NMR (400 MHz, DMSO-*d*$_6$) δ_H = 7.79 (t, *J* = 6.4 Hz, 1H), 7.69 (s, 1H), 7.13-7.07 (dd, *J* = 8.0 Hz, *J* = 7.6 Hz, 2H), 6.88 (d, *J* = 7.4 Hz, 1H), 6.03 (s, 2H), 2.19 (s, 3H); ^{13}C NMR (100 MHz, DMSO-*d*$_6$) δ_C = 156.6, 138.6, 130.5, 127.4, 126.4, 122.5, 121.4, 18.36; Anal. Calcd for $C_8H_{10}N_2O$: C, 63.98; H, 6.71; N, 18.65. Found: C, 63.85; H, 6.61; N, 18.52.

***N*-(4-Chlorophenyl)urea** (Table 2, entry 5): M.p. 208-210 °C; FT-IR (KBr, cm^{-1}) 3427, 3314, 3215, 1654, 1611, 1587, 1549, 1492, 1401, 1357, 1091, 821, 731, 503; ^{1}H NMR (250 MHz, DMSO-*d*$_6$) δ_H = 8.80 (s, 1H), 7.41 (d, *J* = 8.1Hz, 2H), 7.25 (d, *J* = 8.1Hz, 2H), 5.93 (s, 2H); ^{13}C NMR (62.5 MHz, DMSO-*d*$_6$) δ_C = 156.3, 140.1, 128.8, 124.8, 119.6; Anal. Calcd for $C_7H_7ClN_2O$: C, 49.28; H, 4.14; N, 16.42. Found: C, 49.17; H, 4.05; N, 16.31.

***N*-(4-Nitrophenyl)urea** (Table 2, entry 6): M.p. 226-229 °C; FT-IR (KBr, cm^{-1}) 3488, 3381, 3317, 3247, 3218, 3152, 1690, 1595, 1550, 1488, 1414, 1359, 1322, 1299, 1261, 1179, 1111, 1097, 1005, 855, 839, 750, 718, 632, 566, 473, 434, 411; ^{1}H NMR (300 MHz, DMSO-*d*$_6$) δ_H = 9.30 (s, 1H), 8.10 (d, *J* = 9.0Hz, 2H), 7.60 (d, *J* = 9.0Hz, 2H), 6.20 (s, 2H); ^{13}C NMR (75 MHz, DMSO-*d*$_6$) δ_C = 155.7, 147.7, 140.9, 125.5, 117.3; Anal. Calcd for $C_7H_7N_3O_3$: C, 46.41; H, 3.89; N, 23.20. Found: C, 46.52; H, 3.80; N, 23.08.

***N*-(2,5-Dichlorophenyl)urea** (Table 2, entry 7): M.p. 232-234 °C; FT-IR (KBr, cm^{-1}) 3495, 3417, 3364, 3340, 3308, 3206, 2826, 1676, 1610, 1586, 1535, 1466, 1410, 1385, 1351, 1263, 1089, 1056, 873, 805, 792, 764, 583, 557, 475, 440, 418; ^{1}H NMR (300 MHz, DMSO-*d*$_6$) δ_H = 8.24 (s, 2H), 7.38 (d, *J* = 8.1 Hz, 1H), 6.96 (d, *J* = 8.1 Hz, 1H), 6.55 (s, 2H); ^{13}C NMR (75 MHz, DMSO-*d*$_6$) δ_C = 154.7, 137.7, 131.7, 129.9, 121.5, 119.5, 118.8; Anal. Calcd for $C_7H_6N_2OCl_2$: C, 41.00; H, 2.95; N, 13.66. Found: C, 39.84; H, 2.89; N, 13.80.

***N*-(3-Bromophenyl)urea** (Table 2, entry 8): M.p. 141-143 °C; FT-IR (KBr, cm^{-1}) 3375, 3333, 3189, 1679, 1578, 1476, 1410, 1091, 861, 777, 674, 599; ^{1}H NMR (400

MHz, DMSO-d_6) δ_H = 8.74 (s, 1H), 7.83 (s, 1H), 7.23-7.15 (m, 2H), 7.07 (d, J = 8.1 Hz, 1H), 5.97 (s, 2H); ^{13}C NMR (100 MHz, DMSO-d_6) δ_C = 156.2, 142.7, 131.0, 123.0, 120.4, 120.2, 116.8; Anal. Calcd for $C_7H_7N_2OBr$: C, 39.10; H, 3.28; N, 37.16. Found: C, 39.20; H, 3.34; N, 37.26.

***N*-(4-Acethylphenyl)urea** (Table 2, entry 9): M.p. 297-298 °C; FT-IR (KBr, cm^{-1}) 3407, 3307, 3215, 1672, 1613, 1584, 1536, 1508, 1410, 1357,1310, 1273, 1117, 1013, 963, 874, 835, 766, 747, 718, 632, 655, 594, 494, 410; ^{1}H NMR (300 MHz, DMSO-d_6) δ_H = 8.93 (s, 1H), 7.80 (d, J = 8.4 Hz, 2H), 7.50 (d, J = 8.4 Hz, 2H), 6.02 (s, 2H), 2.47 (s, 3H); ^{13}C NMR (75 MHz, DMSO-d_6) δ_C = 196.6, 156.0, 145.7, 130.2, 130.0, 117.0, 26.7; Anal. Calcd for $C_9H_{10}N_2O_2$: C, 60.66; H, 5.66; N, 15.72. Found: C, 60.47; H, 5.45; N, 15.59.

***N*-(1-Naphthyl)urea** (Table 2, entry 10): M.p. 221-222 °C; FT-IR (KBr, cm^{-1}) 3444, 33055, 3206, 3052, 2922, 1651, 1608, 1555, 1530, 1505, 1360, 1335, 1278, 1101, 785, 772, 608, 530; ^{1}H NMR (300 MHz, DMSO-d_6) δ_H = 8.70 (s, 1H), 8.17 (s, 1H), 8.00 (d, J = 7.3 Hz, 1H), 7.85 (s, 1H), 7.73-7.37 (m, 4H), 6.22 (s, 2H); ^{13}C NMR (75 MHz, DMSO-d_6) δ_C = 157.1, 135.9, 134.5, 128.9, 126.6, 126.4, 126.0, 122.7, 122.3, 117.5; Anal. Calcd for $C_{11}H_{10}N_2O_2$: C, 70.95; H, 5.41; N, 15.04. Found: C, 70.82; H, 5.34; N, 14.91.

3. Results and discussion

In this study, *Euphorbia condylocarpa M. bieb* root extract has been used as a reducing and stabilizing agent for the synthesis of silver nanoparticles. Figure 2 and 3 show the UV-Vis and FT-IR spectra of *Euphorbia condylocarpa M. bieb* root extract, respectively.

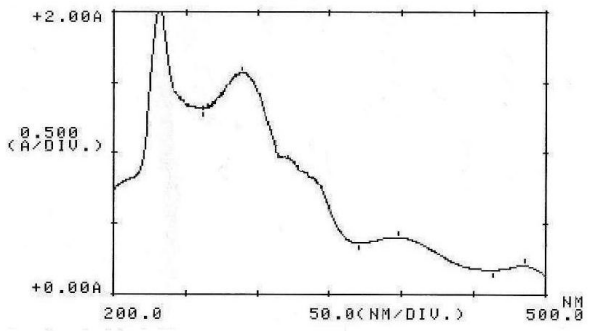

Figure 2. UV-Vis spectrum of *Euphorbia condylocarpa M. bieb* root extract.

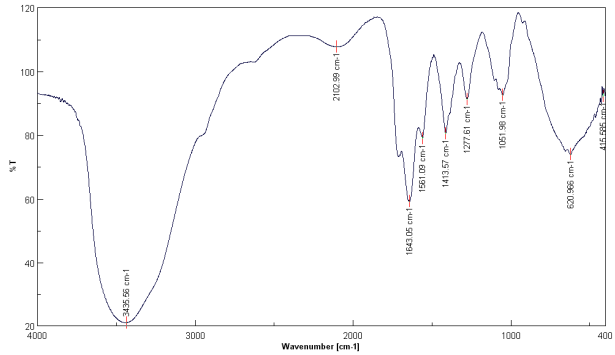

Figure 3. FT-IR spectrum of *Euphorbia condylocarpa M. bieb* root extract.

The UV spectrum with bonds at λ_{max}^{nm} 387 (bond 1) which is due to the transition localized within the B ring of cinnamoyl system; whereas the one depicted at 283 (bond 2) is consistent with absorbance of ring A of benzoyl system (Scheme 2). They are related to the ´ Ÿ ´ transitions and these absorbent bonds demonstrated the presence of flavon nuclei.

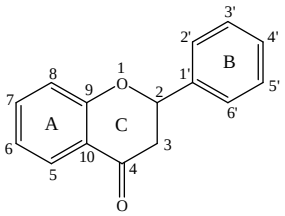

Scheme 2

The FT-IR spectrum depicted some peaks at 3436 to 3000, 1643, 1561, 1413 and 1277 cm^{-1} which represent free OH in molecule and OH group forming hydrogen bonds, carbonyl group (C=O), stretching C=C aromatic ring and C-OH stretching vibrations, respectively.

Reduction of silver ion to silver nanoparticles during exposure to the plant extracts could be followed by color change and spectroscopic techniques such as UV-Vis. As the *Euphorbia condylocarpa M. bieb* root extract was mixed in the aqueous solution of the silver nitrate, it started to change the color from watery to reddish brown (Figure 4) due to the surface Plasmon resonance phenomenon which indicated formation of silver nanoparticles. The intensity of the color was increased during the process.

Figure 4. (a) Photograph of *Euphorbia condylocarpa M. bieb* root extract; (b) Color change of aqueous solution of silver nitrate after addition of *Euphorbia condylocarpa M. bieb* root extract.

Figure 5 shows the UV-Vis spectra of Ag NPs formation. The progression of the reaction, formation and stability of silver nanoparticles were controlled by UV-Vis spectroscopy. The best time was 1 h and the best concentration of $AgNO_3$ was 0.003 M. Also the ratio of plant extract to $AgNO_3$ solution was 1/10. No significant increase in absorbance was observed after 1 h of reaction time, which indicates the completion of reaction. The appearance of a single, bell shaped, surface plasmon band at the wavelength of maximum absorbance at 420 nm, indicated the formation of Ag NPs. The synthesized silver nanoparticles by the this method are quite stable and no obvious variance in the shape, position and symmetry of the absorption peak is observed even after two months which indicates that the as-prepared silver nanoparticles can remain stable.

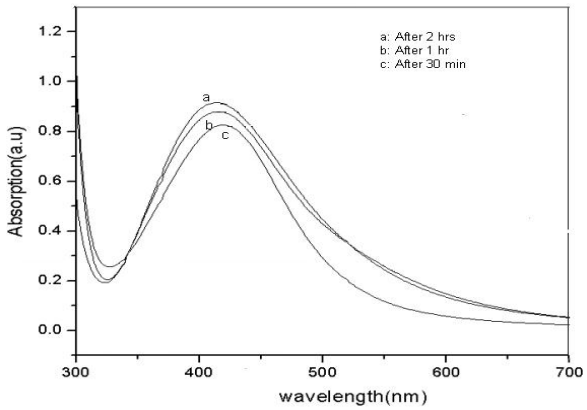

Figure 5. UV-Vis spectrum of green synthesized Ag NPs at different times.

Figures 6 represents the FT-IR spectrum of biosynthesized silver nanoparticles by the *Euphorbia condylocarpa M. bieb* root extract and shows bands at 3423, 2918, 2850, 1578, 1377 and 1033. The band at 3423 cm^{-1} corresponds to free O-H or stretching vibrations of hydroxyl group of alcohols or phenols in bonding. Signals ranging under 3000 to 2800 cm^{-1} identify the methylene stretching bonds. Furthermore, the peak at 1578 cm^{-1} corresponds to conjugated aromatic C=C bonds. As shown in Figure 6, a prominent shift in the wave numbers was observed from 1000 to 1380 cm^{-1} characterize the C-C

stretching bond of hydrocarbon skeletal vibrations. From the analysis of FT-IR bands of silver nanoparticles studies we grasp that the antioxidant polyphenolics have the stronger ability to bind metal indicating that could possibly from the metal nanoparticles (capping of silver nanoparticles) to form biometallic complex (bio chelating) and thereby remove the oxidant agent and stabilize the medium. This suggests that the *Euphorbia condylocarpa* aqueous extract could possibly perform dual functions of formation and stabilization of Ag NPs in the aqueous medium.

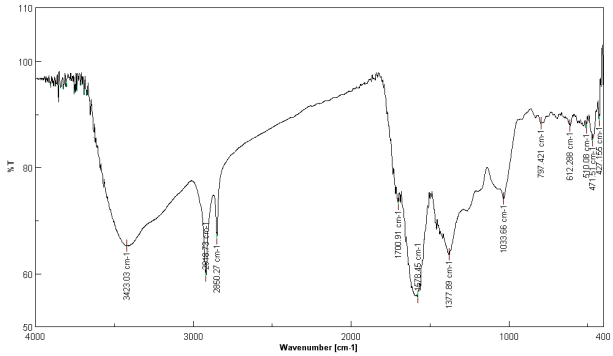

Figure 6. FT-IR spectrum of Ag NPs produced from the root of the *Euphorbia condylocarpa M. bieb* extract.

In Fig. 7, the TEM micrograph of the green silver nanoparticles indicates the nanoparticles are spherical in shape with a narrow size.

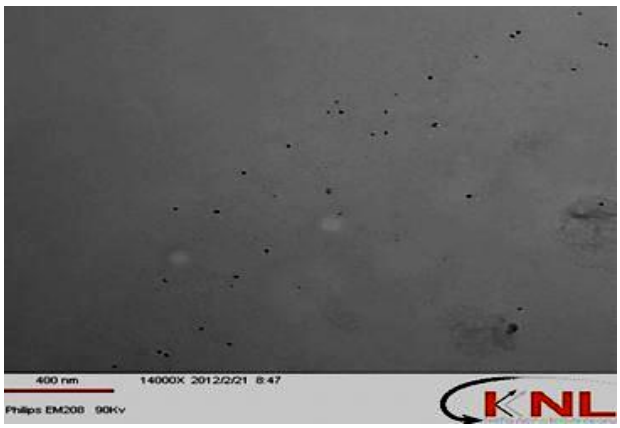

Fig. 7. TEM image of green synthesized Ag NPs.

3.1. Optical modeling

Let us consider a region $0 \le z \le d$ occupied by silver nanoparticles dispersed in water (Figure 8) while the regions $z \le 0$ and $z \ge d$ are vacuous. Suppose an arbitrarily polarized plane wave is normally incident (axial excitation) on the chosen structure from the $z \le 0$. The phasors of incident, reflected and transmitted electric fields are given as [42]:

$$\begin{cases} \underline{E}_{inc}(\underline{r}) = [a_s \underline{u}_y - a_p \underline{u}_x] e^{i K_0 z}, & z \le 0 \\ \underline{E}_{ref}(\underline{r}) = [r_s \underline{u}_y + r_p \underline{u}_x] e^{-i K_0 z}, & z \le 0 \\ \underline{E}_{tr}(\underline{r}) = [t_s \underline{u}_y - t_p \underline{u}_x] e^{i K_0 (z-d)}, & z \ge d \end{cases} \quad (1)$$

where $(a_s, a_p), (r_s, r_p)$ and (t_s, t_p) are the amplitudes of incident plane wave, and reflected and transmitted waves with S- or P-polarizations, $K_0 = \omega\sqrt{\mu_0 \varepsilon_0} = 2\pi / \lambda_0$ is the free space wave number, λ_0 is the free space wavelength, $\varepsilon_0 = 8.854 \times 10^{-12}\ Fm^{-1}$, and $\mu_0 = 4\pi \times 10^{-7}\ Hm^{-1}$ are the permittivity and permeability of free space (vacuum), respectively, and $\underline{u}_{x,y,z}$ are the unit vectors in Cartesian coordinates system.

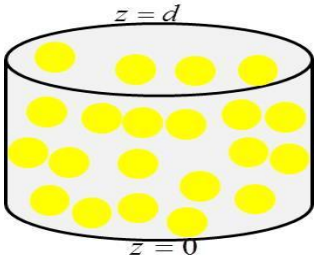

Figure 8. Schematic of the boundary-value problem for silver nanoparticles dispersed in water in order to excitation surface plasmon.

The reflectance and transmittance amplitudes can be obtained, using the continuity of the tangential components of electrical and magnetic fields at interfaces and solving the algebraic matrix equation [43-45]:

$$\begin{bmatrix} t_s \\ t_p \\ 0 \\ 0 \end{bmatrix} = [\underline{\underline{K}}]^{-1} . [\underline{\underline{M}}_{Ag-Water}] . [\underline{\underline{K}}] . \begin{bmatrix} a_s \\ a_p \\ r_s \\ r_p \end{bmatrix} \quad (2)$$

The different terms and parameters of this equation are given in detail by Lakhtakia [42]. In our work the absorption for natural light is considered as $A = \frac{A_S + A_P}{2}$, where

$$A_i = 1.0 - (\sum_{j=s,p} R_{ji} + T_{ji}) ; R_{i,j} = \left| \frac{r_i}{a_j} \right|^2 ; T_{i,j} = \left| \frac{t_i}{a_j} \right|^2 ; i, j = s, p$$

.

In optical modeling, the effective dielectric constant $\varepsilon_{eff} = \varepsilon_W (1 - \frac{3 f (\varepsilon_W - \varepsilon_{Ag})}{2\varepsilon_W + \varepsilon_{Ag} + f(\varepsilon_W - \varepsilon_{Ag})})$ of silver nanoparticles in water was calculated using Maxwell-Garnett theory (MGT), where ε_W and ε_{Ag} are dielectric constants of water and silver, while f is the volume fraction of dispersed material [46]. We have used the bulk experimental refractive indexes silver and water for homogenization [47]. The

calculated optical absorption of structure as a function of wavelength for natural light plane wave at different volume fractions of silver nanoparticles is plotted in Figure 9. The existence of peak in optical absorption of structure at about 400 nm is due to excitation surface plasmon wave [48]. It can be observed that as the volume fraction of nanoparticles increases the width of surface plasmon peak broadens that is consistent with experiment result. By comparison the results of optical modeling and experiment it is seen that there are qualitative agreement between experimental data and results of our applied optical modeling. This slight difference between our optical modeling and experimental result can be related to the structural difference between the idealized theoretical model for structure and that obtained in experimental result. On the other hand, the experimental composite films exhibit a large amount of scattering due to the highly complex and non-ideal structure that the individual nanoparticles exhibit.

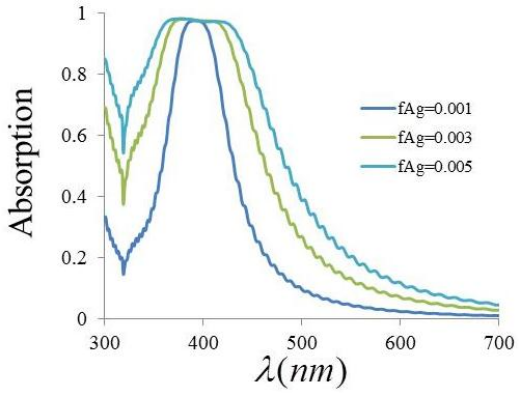

Figure 9. Calculated absorption as a function of wavelength at different volume fractions silver nanoparticles.

3.2. Activity of Ag NPs catalyst for the preparation of N-monosubstituted ureas

In the next step, we tested the catalytic activity of the Ag nanoparticles for the hydration of cyanamides in water. Initial studies were performed in order to optimize the reaction conditions for the hydration of 4-methylphenylcyanamide in the presence of the silver nanoparticles (Table 1). Control experiments show that there is no reaction in the absence of catalyst (Table 1, entry 6). However, addition of the catalyst to the mixture has rapidly increased the synthesis of *N*-monosubstituted ureas in high yields. The best result was obtained with 1.0 mmol of cyanamide, 5.0 mg of Ag NPs and 10 mL of water under reflux conditions, which gave the product in an excellent yield.

Table 1
Hydration of 4-methylphenylcyanamide promoted by silver nanoparticles[a]

Entry	Ag NPs (mg)	Solvent	Time (h)	Yield (%)[b]
1	2	H_2O	4	60
2	4	H_2O	1	80
3	6	H_2O	1	95
4	8	H_2O	1	95
5	6	H_2O:Toluene (8:2 mL)	1	63
6	0	H_2O	4	0

[a] Reaction conditions: cyanamide (1.0 mmol), water (10 mL), Ag NPs (5.0 mg), reflux, 1 h.

[b] Isolated Yield.

Next we examined the utility of the Ag NPs catalyst with other cyanamides (Table 2). Cyanamides contain both electron-releasing and electron-withdrawing groups underwent the conversion in excellent yields. Significantly, the reactions between 1-naphthylcyanamide and water in the presence of Ag NPs afforded corresponding *N*-(1-naphthyl)urea product in excellent yield (Table 2, entry 10).

Table 2
Hydration of different cyanamides by the silver nanoparticles

Entry	Cyanamide	Product	Yield (%)[b]
1	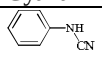	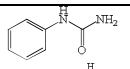	93
2	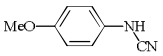	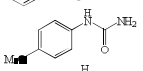	92
3	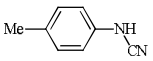	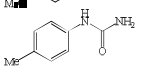	95 (95,94,93)[b]
4	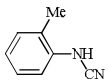	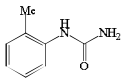	93
5	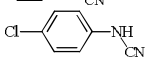	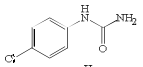	95
6	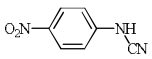	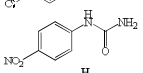	90
7	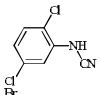	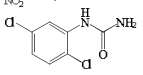	93
8	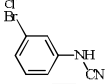	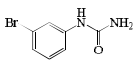	95
9	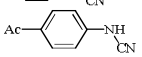	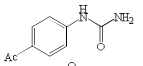	94
10		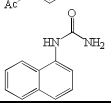	94

[a] Yields are after work-up.

[b] Yield after the fourth cycle.

The first principle of green chemistry states that it is better to prevent waste production than to treat waste or clean it up after it has been created [49]. In all of reported methods in the literature, by-product as waste or pollution is produced. It is not

in compliance with the first principle of green chemistry. In our methods, after completion of the reaction, there is no cyanamide residue in the reaction mixture. Also, no organic solvents were used for the extraction of the product in the work-up step and the method did not require any further purification. Compared to the reported methods, our method is convenient, fast, safe and easy to work-up.

Nevertheless some disadvantages of the literature works are as below:

- The use of organic solvent and toxic and volatile reagents such as phosgene and isocyanates;
- Long reaction times, low yield and harsh reaction conditions;
- The use of Flash chromatography or recrystallization for purification of the products;
- The use of corrosive acids or bases;
- The use of homogeneous catalysts;
- Several-step methods.

All above items are wasting money and time consuming, so our proposed method can be considered as a green protocol which the reaction will take place at room temperature with high atom economy, high yields and easy operations without application of toxic organic solvents, bases, acids and expensive reagents or catalysts. Compared with the other literature works on the synthesis of *N*-monosubstituted ureas, the notable features of our method are:

- The reaction system is simple;
- Organic solvents are not needed;
- Brønsted acids and organic reagents such as acetaldoxime are not needed;
- The use of water as a green solvent;
- The yields of the products are very high;
- The use of plant extract as an economic and effective alternative represents an interesting, fast and clean synthetic route for the large scale synthesis of silver nanoparticles;
- The Ag NPs catalyst can be easily recovered;
- High reaction pressure are avoided; and;
- No side product was observed under the reaction conditions, thus this method did not require any further purification.

The second principle of green chemistry states that the synthetic systems should be focused to improve the atom economy or atom efficiency [49]. Atom economy (AE) is a useful concept for estimating the environmental impacts of starting materials in a reaction to reach a desired product [50]. In comparison with of the literature works, atom economy of our work is very excellent.

To the best of our knowledge, Ag NPs catalyst is one of the most general and active catalysts reported so far for the synthesis of *N*-monosubstituted ureas. The Ag NPs

catalyst has an important role in promotion of the synthesis of *N*-monosubstituted ureas as a Lewis acid. The catalyst may show complexation towards nitrile group of cyanamides and thus may enhance the electrophilic character. It involves activation of the nitrile group over surface of the catalyst and subsequent nucleophilic attack of the water.

The products were characterized by IR, ^{1}H NMR and ^{13}C NMR spectroscopy and from melting points. The disappearance of one strong and sharp absorption band (CN stretching band), and the appearance of NH, NH_2 and C=O stretching bands in the IR spectra, were evidence for the formation of *N*-monosubstituted ureas (Figure 10). The ^{1}H NMR spectra of the products showed one NH proton signal and another signal for the NH_2 protons (Figure 11). ^{13}C NMR spectra displayed signal for the CO carbon.

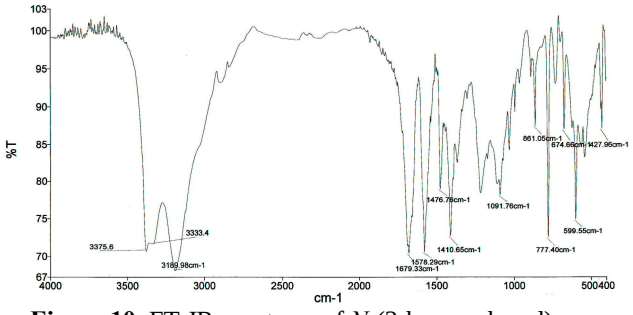

Figure 10. FT-IR spectrum of *N*-(3-bromophenyl)urea.

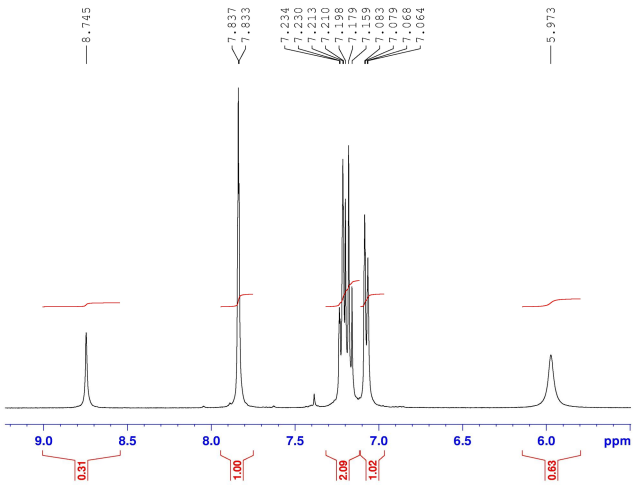

Figure 11. ^{1}H NMR spectrum (400 MHz, DMSO-d_6) of 5-(3-bromophenyl)urea.

3.3. Catalyst recyclability

The catalyst recycling is an important step as it reduces the cost of the process. The reusability of the catalyst was checked in the reaction of 4-methylphenylcyanamide with water under the present reaction conditions (Table 2, entry 3). After the completion of the reaction, Ag nanoparticles were separated from the reaction mixture by centrifugation. The catalyst was washed with water several times, dried and employed for the next

reaction. The activity of the four consecutive runs (95%, 95%, 94% and 93%) revealed the practical recyclability of the applied catalyst. This reusability demonstrates the high stability and turnover of catalyst under operating conditions.

4. Conclusions

In summary, we synthesized silver nanoparticles with *Euphorbia condylocarpa M. bieb* root extract as a reducing and stabilizing agent without application of toxic reagents or surfactant template. The optical properties and catalytic activity of the silver nanoparticles were also studied. This fast and green synthetic method has the advantages of high yields, elimination of homogeneous catalysts, simple methodology, easy preparation and handling of the catalyst and easy work up. The Ag NPs is eco-friendly catalyst because it produces little waste, and can be recovered and successively reused without the significant loss of activity. The synthesized silver nanoparticles by this method are quite stable and can be kept under inert atmosphere for several months.

Acknowledgements

We gratefully acknowledge from the Iranian Nano Council and University of Qom for the support of this work.

References

[1] A. Tsopmo, D. Ngnokam, D. Ngamga, J.F. Ayafor, O. Sterner, J. Nat. Prod. 62 (1999) 1435.
[2] K. Matsuda, Med. Res. Rev. 14 (1994) 271.
[3] V. Papesch, E.F. Schroeder, J. Org. Chem. 16 (1951) 1879.
[4] R.L. Clark, A.A. Pessolano, J. Am. Chem. Soc. 80 (1958) 1658.
[5] K. Burgess, J. Ibarzo, S.D. Linthicum, D.H. Russell, H. Shin, A. Shitangkoon, R. Totani, A.J. Zhang, J. Am. Chem. Soc. 119 (1997) 1556.
[6] S. Knapp, J.J. Hale, M. Bastos, A. Molina, K.Y. Cheng, J. Org. Chem. 57 (1992) 6239.
[7] X. Peng, F. Li, C. Xia, Synlett (2006) 1161.
[8] B. Zhu, R.J. Angelici, J. Am. Chem. Soc. 128 (2006) 14460.
[9] P.-A. Enquist, P. Nilsson, J. Edin, M. Larhed, Tetrahedron Lett. 46 (2005) 3335.
[10] F. Bigi, R. Maggi, G. Sartori, Green Chem. 2 (2000) 140.
[11] E. Wertheim, J. Am. Chem. Soc. 53 (1931) 200.
[12] V.D. Jadhav, E. Herdtweck, F.P. Schmidtchen, Chem. Eur. J. 14 (2008) 6098.
[13] D. Schade, K. Topker-Lehmann, J. Kotthaus, B. Clement, J. Org. Chem. 73 (2008) 1025.
[14] G. Haufe, U. Rolle, E. Kleinpeter, J. Kivikoski, K. Rissanen, J. Org. Chem. 58 (1993) 7084.
[15] B.B. Snider, J.R. Duvall, Org. Lett. 7 (2005) 4519.
[16] E. Artuso, I. Degani, R. Fochi, C. Magistris, Synthesis (2007) 3497.
[17] S.H. Kim, B.R. Park, J.N. Kim, Bull. Korean Chem. Soc. 32 (2011) 716.
[18] P.E. Savage, Chem. Rev. 99 (1999) 603.
[19] M. Watanabe, T. Sato, H. Inomata, R.L.Jr. Smith, K. Arai, A. Kruse, E. Dinjus, Chem. Rev. 104 (2004) 5803.
[20] M.C. Daniel, D. Astruc, Chem. Soc. Rev. 104 (2004) 293.
[21] T. Sun, K. Seff, Chem. Rev. 94 (1994) 857.
[22] L.T. Chang, C.C. Yen, J. Appl. Polym. Sci. 55 (1995) 371.
[23] A.L. Stepanov, V.N. Popok, I.B. Khaibullin, U. Kreibig, Nucl. Instr. Meth. B 191 (2002) 473.

[24] P. Matejka, B. Vlckova, J. Vohidal, P. Pancoska, V. Baumrunk, J. Phys. Chem. 96 (1992) 1361.
[25] F. Martinez-Gutierrez, P.L. Olive, A. Banuelos, E. Orrantia, N. Nino, E. Sanchez, Nanomedicine 6 (2010) 681.
[26] R.P. Andres, J. Bielefield, J.L. Henderson, O.B. Janes, V.K. Kolayunta, C.P. Kubiak, W.J. Maloney, R.P. Osifachin, J. Science 273 (2006) 1690.
[27] S. Anilkumar, M. Kazeman, G. Suabha, 2007, www.Springer.com.
[28] J.P. Kottmann, J.F. Martin, D.R. Smith, S. Schultz, Phys. Rev. B 64 (2002) 235402.
[29] E.S. Abdel-Halim, M.H. El-Rafie, S.S. Al-Deyab, Carbohydr. Polym. 85 (2011) 692.
[30] S.S. Shankar, A. Ahmad, M. Sastry, Biotechnol. Prog. 19 (2003) 1627.
[31] S.P. Dubey, M. Lahtinen, M. Sillanpa, Process Biochem. 45 (2010) 1065.
[32] D. Philip, Spectrochim. Acta, Part A 73 (2009) 374.
[33] A. Rizk, Bot. J. Linn. Soc. 94 (1987) 293.
[34] A.R. Jasbi, Phytochem. 67 (2006) 1977.
[35] Y.V. Roshchin, N.P. Kir'yalov, Chem. Nat. Compd. 6 (4) (1970) 501.
[36] M. Nasrollahzadeh, S.M. Sajadi, M. Maham, P. Salaryan, A. Enayati, S.A. Sajjadi, K. Naderi, Chem. Nat. Compd. 47 (2011) 434.
[37] D. Habibi, M. Nasrollahzadeh, T.A. Kamali, Green Chem. 13 (2011) 3499.
[38] D. Habibi, M. Nasrollahzadeh, H. Sahebekhtiari, S.M. Sajadi, Synlett 23 (2012) 2795.
[39] H. Shahroosvand, L. Najafi, E. Mohajerani, A. Khabbazi, M. Nasrollahzadeh, J. Mater Chem. C 1 (2013) 1337.
[40] D. Habibi, M. Nasrollahzadeh, A.R. Faraji, Y. Bayat, Tetrahedron 66 (2010) 3866.
[41] D. Habibi, M. Nasrollahzadeh, Monatsh. Chem. 143 (2012) 925.
[42] A. Lakhtakia, R. Messier, Sculptured thin films, Nanoengineered Morphology and Optics. SPIE, USA, 2005.
[43] J.A. Polo Jr, A. Lakhtakia, Proc. R. Soc. A456 (2009) 87.
[44] A. Lakhtakia, Optics. Commun. 279 (2007) 291.
[45] F. Babaei, M. Omidi, Plasmonics 8 (2013) 1051.
[46] A. Garahan, L. Pilon, J. Yin, J. Appl. Phys. 101 (2007) 014320.
[47] E.D. Palik, Handbook of Optical Constants of Solids, Academic Press, New York, USA, 1985.
[48] M. Mansuripur, A.R. Zakharian, J.V. Moloney, Opt. Photon. News 18 (2007) 44.
[49] P.T. Anastas, J.C. Warner. Green Chemistry: Theory and Practice, Oxford University Press, New York, 1998, p. 30.
[50] R.A. Sheldon, Pure Appl. Chem. 72 (2000) 1233.

Graphical Abstract

Green synthesis, optical properties and catalytic activity of silver nanoparticles in the synthesis of *N*-monosubstituted ureas in water

Mahmoud Nasrollahzadeh*, Ferydon Babaei, S. Mohammad Sajadi and Ali Ehsani

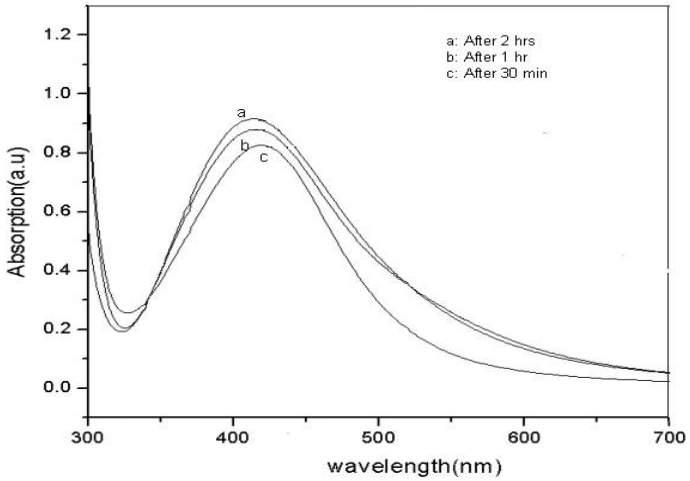

Figures caption:

Figure 1. Image of *Euphorbia condylocarpa M. bieb*.

Figure 2. UV-Vis spectrum of *Euphorbia condylocarpa M. bieb* root extract.

Figure 3. FT-IR spectrum of *Euphorbia condylocarpa M. bieb* root extract.

Figure 4. (a) Photograph of *Euphorbia condylocarpa M. bieb* root extract; (b) Color change of aqueous solution of silver nitrate after addition of *Euphorbia condylocarpa M. bieb* root extract.

Figure 5. UV-Vis spectrum of green synthesized Ag NPs at different times.

Figure 6. FT-IR spectrum of Ag NPs produced from the root of the *Euphorbia condylocarpa M. bieb* extract.

Figure 7. TEM image of green synthesized Ag NPs

Figure 8. Schematic of the boundary-value problem for silver nanoparticles dispersed in water in order to excitation surface plasmon.

Figure 9. Calculated absorption as a function of wavelength at different volume fractions silver nanoparticles.

Figure 10. FT-IR spectrum of *N*-(3-bromophenyl)urea.

Figure 11. ^{1}H NMR spectrum (400 MHz, DMSO-d_6) of 5-(3-bromophenyl)urea.

Figure 1. Image of *Euphorbia condylocarpa M. bieb*.

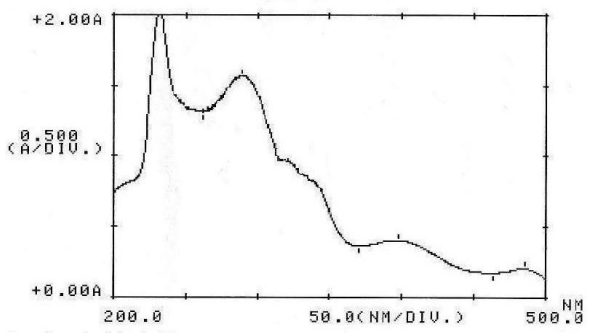

Figure 2. UV-Vis spectrum of *Euphorbia condylocarpa M. bieb* root extract.

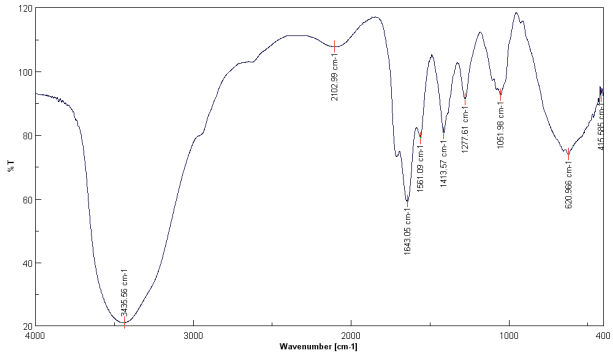

Figure 3. FT-IR spectrum of *Euphorbia condylocarpa M. bieb* root extract.

Figure 4. (a) Photograph of *Euphorbia condylocarpa M. bieb* root extract; (b) Color change of aqueous solution of silver nitrate after addition of *Euphorbia condylocarpa M. bieb* root extract.

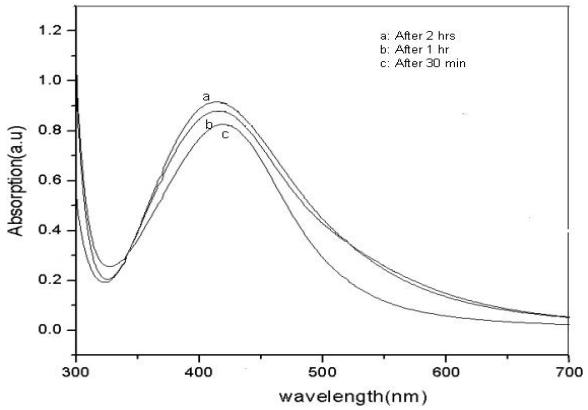

Figure 5. UV-Vis spectrum of green synthesized Ag NPs at different times.

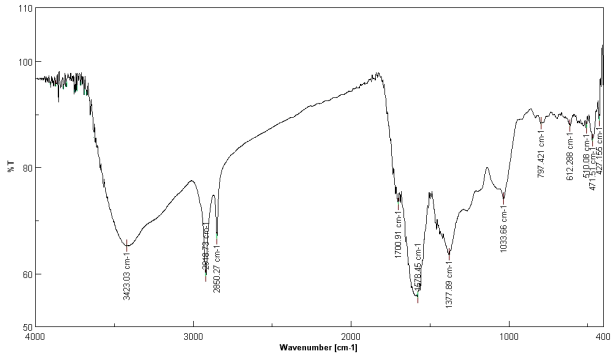

Figure 6. FT-IR spectrum of Ag NPs produced from the root of the *Euphorbia condylocarpa M. bieb* extract.

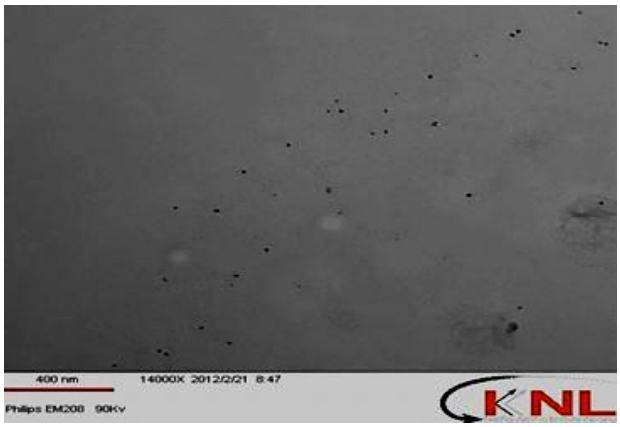

Fig. 7. TEM image of green synthesized Ag NPs.

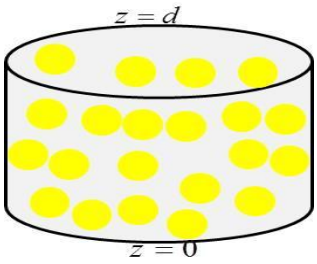

Figure 8. Schematic of the boundary-value problem for silver nanoparticles dispersed in water in order to excitation surface plasmon.

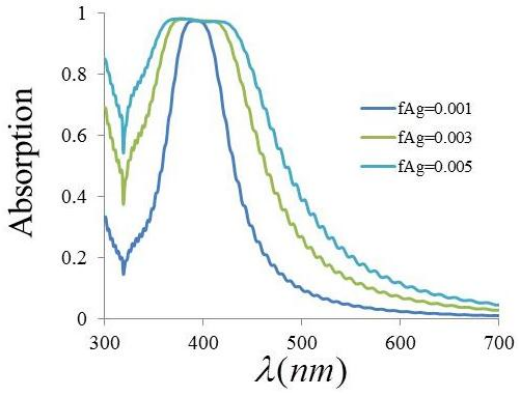

Figure 9. Calculated absorption as a function of wavelength at different volume fractions silver nanoparticles.

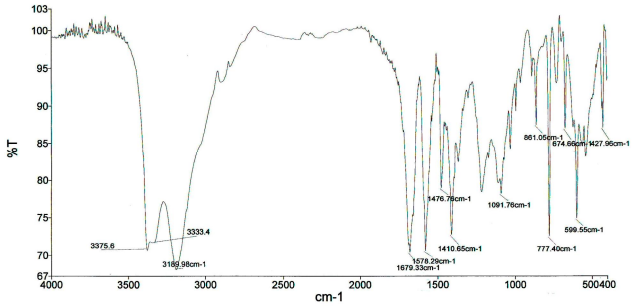

Figure 10. FT-IR spectrum of *N*-(3-bromophenyl)urea.

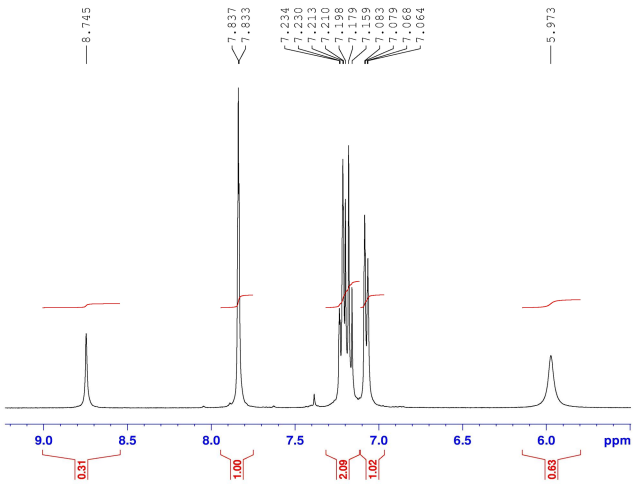

Figure 11. ^{1}H NMR spectrum (400 MHz, DMSO-d_6) of 5-(3-bromophenyl)urea.